Food Chemistry 493 (2025) 145826

Contents lists available at ScienceDirect

Food Chemistry

journal homepage: www.elsevier.com/locate/foodchem

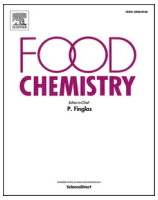

Reinforcement of chitosan/ polyvinyl alcohol film by quercetin self-assembled nanocrystals for fresh meat preservation

Simin Fan [a,b,c], Wenxin Wang [a], Qingfeng Yang [a], Chaoqiao Zhu [a], Ming Tian [a], Aurore Richel [b], Marie-Laure Fauconnier [c], Chengli Hou [a,d,*], Dequan Zhang [a]

[a] Institute of Food Science and Technology, Chinese Academy of Agricultural Sciences, Key Laboratory of Quality, Safety, Collection, Storage, Transportation and Control of Agricultural Products, Ministry of Agriculture and Rural Affairs, Beijing 100193, China
[b] Laboratory of Biomass and Green Technologies, Gembloux Agro-Bio Tech, University of Liège, Passage de Déportés 2, Gembloux 5030, Belgium
[c] Laboratory of Chemistry of Natural Molecules, Gembloux Agro-Bio Tech, University of Liège, Passage de Déportés 2, Gembloux 5030, Belgium
[d] Institute of Western Agriculture, Chinese Academy of Agricultural Sciences, Changji 831100, China

ARTICLE INFO

Keywords:
Active packaging
Chitosan/ polyvinyl alcohol film
Quercetin nanocrystals
Molecular dynamics simulation
Meat preservation

ABSTRACT

The development of sustainable and functional food packaging is essential for mitigating food waste. In this study, quercetin nanocrystals (QNs) are synthesized and utilized to improve functionality of chitosan/ polyvinyl alcohol (PC) films. Molecular dynamics simulations and experimental characterizations reveal that the self-assembly of QNs is primarily driven by supramolecular interactions. QNs exhibit good compatibility with PC films, acting both as a nanofiller to improve mechanical properties (tensile strength of 49.68 MPa and elongation at break of 176.02 %) and as an active agent to impart antioxidant properties (fourfold increase compared to plain PC film). Additionally, QNs enhance the thermal stability, UV-blocking capability, and water vapor barrier properties of the PC films. More importantly, the QNs-reinforced PC films significantly extend the shelf life of fresh meat to 11 days. This work provides an effective strategy for fabricating eco-friendly and functional food packaging materials, demonstrating great potential for application in food preservation.

1. Introduction

Packaging materials account for approximately 40 % of global plastic production, with food packaging being the primary application (Shlush & Davidovich-Pinhas, 2022). This substantial usage contributes significantly to resource depletion, environmental pollution, ecosystem disruption, and health risks, which has become one of the major issues of global concern. These pressing issues have driven researchers to explore next-generation materials that align with the sustainability goals of the food packaging industry (Ning et al., 2025; Peydayesh et al., 2024; Thakur et al., 2018; Wang, Xue, et al., 2024). Biopolymers, combining sustainable and biodegradable properties such as chitosan (CS), cellulose, gelatin, and zein, have drawn increasing interest as promising alternatives to traditional fossil-based and non-biodegradable plastics (Uysal-Unalan et al., 2024).

CS is a linear polysaccharide derived from chitin, commonly found in crustacean shells and insect exoskeletons. It is produced through the *N*-deacetylation of chitin, yielding abundant amino groups and a unique structural organization, which distinguishes it from other polysaccharides (Wang & Zhuang, 2022). As a prominent natural biopolymer, CS has excellent film-forming properties and biocompatibility, making it highly promising for creating bio-based film materials (Fan et al., 2023). Nevertheless, the limited water resistance of pure CS film restricts its wider use in food packaging, a challenge that can be mitigated by integrating polyvinyl alcohol (PVA) (Zhang, Khan, et al., 2024). PVA is synthesized through non-fossil routes and can be fully biodegraded into water and carbon dioxide by specific microorganisms. PVA and CS interact through intermolecular hydrogen bonding, creating a robust composite network with enhanced mechanical properties (Jiang et al., 2023; Wang, Chen, et al., 2024; Yang et al., 2023). This integration mitigates film deformation caused by the hydrophilic nature of CS, effectively addressing its limitations. Imparting bioactivity, such as antioxidant and antimicrobial properties, to the PC composite film can further enhance its effectiveness in ensuring food safety and extending the shelf life of packaged foods. It has been reported that several studies have incorporated active substances such as titanium

* Corresponding author at: Institute of Food Science and Technology, Chinese Academy of Agricultural Sciences, Key Laboratory of Quality, Safety, Collection, Storage, Transportation and Control of Agricultural Products, Ministry of Agriculture and Rural Affairs, Beijing 100193, China.
E-mail address: houchengli@caas.cn (C. Hou).

https://doi.org/10.1016/j.foodchem.2025.145826
Received 20 February 2025; Received in revised form 23 July 2025; Accepted 3 August 2025
Available online 6 August 2025

dioxide (Wang, Yang, et al., 2024), zinc oxide (Sultan et al., 2024), and silver nanoparticles (D. Yang et al., 2023) into PC composite films. However, these additives may pose potential risks to human health and the environment. Furthermore, the weak interactions and inadequate compatibility between these active substances and PC composite films often result in compromised mechanical properties. Therefore, green and effective materials that simultaneously enhance the mechanical properties and stabilize the bioactivity of PC composite films are needed to achieve a better balance between multiple performance indicators.

Quercetin is a natural polyphenol with a flavonoid structure, confirmed to possess potent antioxidant and antimicrobial properties (Kandemir et al., 2022; Luo et al., 2025). The bioactive properties of quercetin have been utilized to develop various biopolymer-based food active films, demonstrating significant potential in preserving food freshness. However, the limited water solubility of quercetin results in poor dispersibility within the hydrophilic film-forming solution, compromising the density and structural integrity of the composite film. Recently, self-assembly nanotechnology has emerged as a promising strategy to enhance natural substances by improving their poor water dispersibility and stability, and preserving their bioactivity (Guo et al., 2024). In addition, self-assembled nanoparticles can act as efficient nanofillers, strengthening the interfacial interactions between polymers and increasing the entanglement of molecular chains, thereby positively influencing the mechanical properties of the film (Ma et al., 2022; Priyadarshi et al., 2022). Hydrophobic quercetin molecules can self-assemble under specific conditions to form nanoparticles, known as quercetin nanocrystals (QNs) (Chenxi et al., 2025), which enhance the water dispersibility of raw quercetin (Guo et al., 2024; Li et al., 2023; Manca et al., 2020). Building on these findings, this study assembles quercetin into QNs, creating a nanofiller with enhanced dispersibility to improve the functional properties of PC composite films.

In this work, we developed QNs and simulated their self-assembly process, validating the results through various characterizations. The QNs were then incorporated into PC polymer matrices to fabricate functional packaging films using a solution casting method. The influence of QNs on the microstructure, mechanical strength, UV resistance, barrier properties, and antioxidant activity of PC film was thoroughly investigated. Their potential application was further demonstrated by using the films to wrap fresh meat. This study provides valuable insights for the development of QN-reinforced PC composite films as high-performance active packaging for food preservation.

2. Experimental section

2.1. Materials

Quercetin was bought from Shanghai Yuanye Bio-Technology Co., Ltd. (Shanghai, China). Chitosan with a deacetylation degree ≥95 % and polyvinyl alcohol (Mw31000–50,000, alcoholysis degree 98–99 %) were obtained from Macklin Biochemical Technology Co., Ltd. (Shanghai, China). Absolute ethyl alcohol and glycerol were procured by Sinopharm Chemical Reagent Co., Ltd. (Shanghai, China). 2,2′-azino-bis (3-ethylbenzothiazoline-6-sulfonic acid) (ABTS) free radical scavenging capacity assay kits were obtained from Solarbio Science & Technology Co., Ltd. (Beijing, China). Trichloroacetic acid was obtained from Shanghai Aladdin Biochemical Technology Co., Ltd. (Shanghai, China). Plate count agar was provided by Beijing Land Bridge Technology Co., Ltd. (Beijing, China). All reagents used in this study were of analytical grade.

2.2. Preparation and characterization of QNs

The QNs were prepared according to the method (Li et al., 2023) with some modifications. In brief, 200 mg of quercetin was dissolved in 10 mL absolute ethanol. Then, the quercetin-alcohol solution was added dropwise to ninefold volume pre-chilled water under ultrasonic treatment (45 W) for crystallization. Finally, 2 mg/mL QNs solution was obtained and stored at 4 °C for further use.

The characterization details of QNs including FTIR, fluorescence spectra, and UV–*v*is absorption spectra were provided in the supplementary information.

2.3. Preparation of QNs-reinforcement PC composite film (PC@QNs)

The PC@QNs composite films were fabricated by casting technique. Firstly, CS powder was dissolved in acetic acid aqueous solution (2 %, *v*/v) at 50 °C and PVA powder was dissolved in ultrapure water at 90 °C, respectively. After complete dissolution, the CS solution (1.5 wt%) was mixed with isovolumetric PVA solution (2 wt%). Then, 30 wt% glycerol was added to the above mixture to form a film-forming solution. Subsequently, various percentages (0 %, 5 %, 10 %, 15 %) of QNs solution (2 mg/mL) were blended uniformly with a film-forming solution. Finally, 20 mL of prepared mixture was poured onto a 90 mm plastic plate and dried at 50 °C for 12 h. The obtained films were labeled as PC, PC@QNs1, PC@QNs2, and PC@QNs3, respectively. Before further characterization, all films were conditioned at 50 % relative humidity and room temperature.

2.4. Characterization of PC@QNs

2.4.1. Morphology

Scanning Electron Microscope (SEM): The surface and cross-section microtopography of PC@QNs were analyzed using an SU 1510 SEM (Hitachi, Japan). Before observation, the films were frozen and treated with liquid nitrogen to obtain cross-sectional parts.

2.4.2. Structural characterization

Fourier-transform infrared spectroscopy (FTIR), X-Ray diffraction (XRD), and thermal gravimetric (TG) analysis. The FTIR spectra of the PC@QNs were recorded using a Tensor 27 FTIR spectrophotometer (Bruker, Germany), and the XRD patterns were conducted using an Ultima IV X-ray diffractometer (Rigaku, Japan). The thermal degradation curve of PC@QNs was obtained using Pyris Diamond TG/DTA thermogravimetric analyzer (PerkinElmer Inc., USA). Before heated, the film sample (5.0 ± 0.5 mg) was weighed and sealed in aluminum pans. The temperature was programmed to increase from 30 to 500 °C at a rate of 10 °C/min under a nitrogen atmosphere.

2.4.3. Mechanical property

The tensile strength and elongation at the break of PC@QNs were measured using a TA-XT Plus texture analyzer (Stable Micro System Co., Ltd., UK) by following the set program (Fan et al., 2023). Specifically, the film was cut into an 80 mm × 10 mm rectangle and secured in the clamp. The initial grip separation was set to 50 mm, with a stretching speed of 50 mm/min. Before measurement, the thickness of PC@QNs was examined at five random locations.

2.4.4. Optical properties

The light transmittance of the PC@QNs was measured using a UV–visible spectrophotometer (UV-6000PC, Metash, China). Before measurement, the film was cut into a 40 mm × 10 mm strip and placed in the sample tank for analysis.

2.4.5. Water vapor and oxygen barrier performance

The water vapor permeability (WVP) and oxygen permeability (OP) of PC@QNs were tested according to a previous procedure (Wang, Yang, et al., 2024).

2.4.6. Antioxidant properties

The DPPH and ABTS free radical scavenging methods were employed to evaluate the antioxidant properties of PC@QNs. 200 mg of a film sample was soaked in 10 mL 95 % (*v*/v) ethanol for 12 h. The 10 μL

extraction solution mentioned above was taken and mixed with 190 uL DPPH work solution (0.1 mM DPPH-ethanol solution), and then reacted for 30 min in the dark, the absorbance of the mixture was determined at 517 nm. For ABTS radical scavenging, an appropriate amount of film sample solution was mixed with 190 μL ABTS work solution (7.4 mM ABTS-water solution and 2.6 mM $K_2S_2O_8$-water solution). After being incubated in darkness for 30 min, the absorbance of the mixture was determined at 734 nm.

2.5. Molecular dynamics (MD) simulation

The self-assembly behavior of quercetin in aqueous solution was explored by using MD simulation (Fu et al., 2024; Hu et al., 2024; Wang et al., 2023). A simulation system was constructed in a box of 10 nm × 10 nm × 10 nm, containing 10 randomly placed quercetin molecules, labeled as system A. System A was solvated with water molecules, ensuring proper solvation without steric clashes. After construction, energy minimization was performed to eliminate unfavorable interactions, followed by applying periodic boundary conditions in all three directions. System A was then equilibrated at constant temperature (298 K) and constant pressure (1 atm) using the *V*-rescale autotuning algorithm. Subsequently, a 10 ns equilibration under the NPT ensemble was conducted with a 2 fs timestep. Finally, a 100 ns MD simulation under the same NPT conditions was conducted. The visualization of structures was performed by VMD software.

To further investigate the intermolecular interactions between QNs (quercetin aggregates) and PC polymers, another simulation system was constructed and named as system B (Ning, et al.). System B consisted of CS chains, PVA chains, and the quercetin aggregates from the final state of System A. After constructing the simulation system B, energy minimization was performed, and periodic boundary conditions were applied in all three directions. The simulation underwent a 10 ns NPT ensemble simulation with a three-step temperature process: the temperature was gradually increased from 298 K to 323 K over the first 0.5 ns, maintained at 323 K for 8.5 ns, then decreased to 298 K over 0.5 ns, and finally stabilized at 298 K for 0.5 ns. Subsequently, a 50 ns molecular dynamics simulation was performed under NPT ensemble conditions.

2.6. Assessment of ecological and economic cost

The impact of producing PC@QNs was evaluated by life cycle assessment method described in reference (Wang, Yang, et al., 2024). The database used was Ecoinvent 3.9, the calculation method selected was Recipe 2016 midpoint, and the calculation software was Simapro 9.5. The economic cost of producing PC@QNs was calculated by comparing films made from polyethylene film, and polypropylene film based on publicly available data.

2.7. Application for meat preservation

The *Longissimus dorsi* muscles of pork meat was obtained from Beijing Ershang Meat Food Group Co., Ltd. (Beijing, China). The meat sample was cut into cuboid shapes weighing 50 ± 5 g and placed at the bottom of a polypropylene-based tray containers (6 cm × 3 cm), and the experimental film (PC@QNs) was used as the top covering film. Commercial polyethylene (PE) packaging film (15,000 cm^3/ m^2■day ■0.1 MPa) was used as control. The same contact configuration was applied in the PE group (control group) to ensure a valid comparison, with the only variable being the type of covering film. The packaged pork meat samples were stored in a refrigerator at 4 °C. The total viable count (TVC) of pork meat samples was determined with slight modifications based on the previously described method (Fan et al., 2024). Briefly, 5.0 ± 0.5 g of the meat sample was placed in 45 mL of sterile saline solution in aseptic bags. The extract was then serially diluted by a factor of 10 using a sterile saline solution. Finally, 100 μL of the diluted extract was spread onto plate count agar and incubated at 37 °C for 48 h. The total *v*olatile basic nitrogen analysis (TVB-N) of pork meat samples was determined based on the procedure in reference (Gu et al., 2023). The TVB-N of pork meat samples was measured using the auto-Kjeldahl device (K9840, Hanon Instruments, Jinan, China). Before measurement, the pork meat sample was minced and soaked in 2 % (*w/v*) trichloroacetic acid solution for 8 h.

2.8. Statistical analysis

The experiments were conducted in triplicate, and the results were presented as mean ± standard deviation (SD). Statistical analysis was performed using SPSS Statistics V26.0 software (IBM Corp., Armonk, New York, USA). Analysis of variance (ANOVA) and Duncan's multiple range test were applied to evaluate the significance of differences, with $P < 0.05$ considered statistically significant.

3. Results and discussion

3.1. Preparation and characterization of QNs

3.1.1. Multispectral analysis

FTIR spectra of raw quercetin and QNs were compared in Fig. 1a. The characteristic peaks near 3330 cm^{-1} correspond to O—H stretching vibrations, which exhibited a slight shift to lower wavenumbers, suggesting the formation of hydrogen bonds in QNs. The characteristic peaks were observed at 1640 cm^{-1} and 1530 cm^{-1}, which were attributed to the stretching vibrations of aromatic rings (Yang et al., 2024), and the slight broadening of these peaks suggested the formation of π-π conjugation effect (Fu et al., 2024). The characteristic peaks displayed in the UV–vis spectra (Fig. 1b) revealed the molecular interactions during the preparation of QNs. Specifically, the characteristic bands in the range of 240–290 nm and 300–450 nm were attributed to the A-ring benzoyl and B-ring cinnamoyl systems, respectively (Li et al., 2023). These bands exhibited broadening and shifts in QNs compared to raw quercetin, indicating changes in the electronic environment and enhanced molecular interactions. Subsequently, the fluorescence spectra of QNs were investigated (Fig. 1c). The fluorescence emission peak at 580 nm, described as keto emission, was enhanced during the preparation of QNs, indicating the formation of molecular aggregation (He et al., 2018).

3.1.2. MD simulations

To better understand the process of self-assembly of QNs, it was analyzed by MD simulations. Fig. 1d illustrates the aggregation behavior observed during the production simulation process. Initially, the quercetin molecules were randomly distributed in a cubic box, then the quercetin molecules self-assembled into fibrous nanoclusters. After 100 ns, all quercetin molecules self-organized and formed a stable nanofiber cluster structure. Fig. 1e showed the representative interactions in fibrous nanoclusters, where the benzene ring formed a π–π stacking structure and the polyphenol hydroxyl formed hydrogen bonds. The solvent-accessible surface area (SASA) describes the molecular surface area that can be accessed by solvent molecules. During the self-assembly process, the SASA decreased significantly from 68.76 nm^2 to 30.73 nm^2 (Fig. 1f), indicating tighter molecular packing. Despite the reduced surface area, the improved water solubility of QNs likely results from higher surface polarity and lower aggregation tendency.

In short, quercetin molecules self-assembled in aqueous solution through various supramolecular interactions. Starting from an initially disordered dispersion, the quercetin molecules aggregated under the influence of water molecules, forming an extensive hydrogen bonding network. This facilitated the formation of ordered, stacked nanofibrous clusters. Additionally, hydrophobic interactions and π-π stacking further stabilized the assemblies.

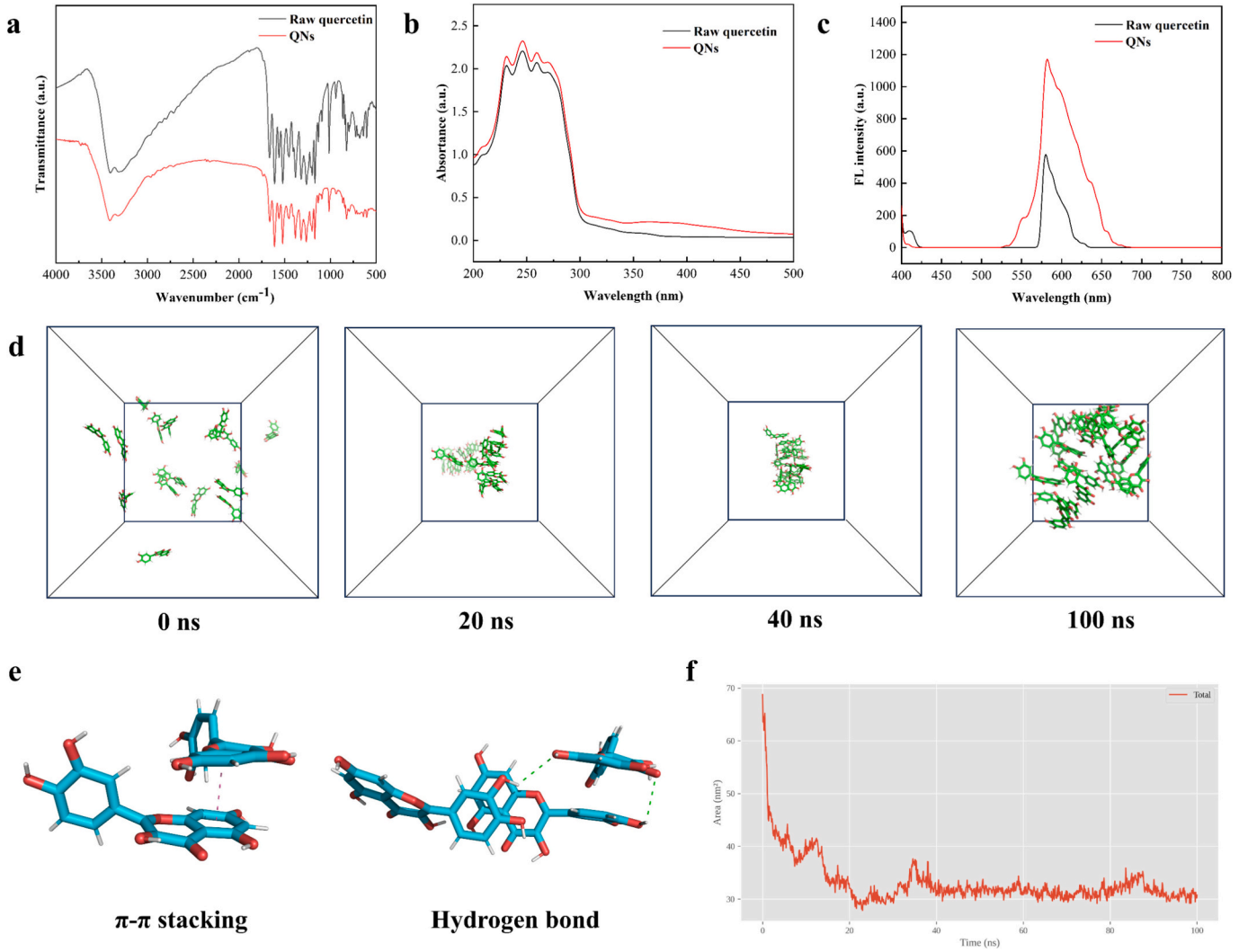

Fig. 1. Characterization of the quercetin nanocrystals (QNs). FTIR spectra (a), UV–vis absorption spectra (b), and fluorescence spectra (c) of QNs. Molecular dynamics simulations of QNs, structural changes of the QNs system during the simulation (d), molecular interactions of the QNs (e), and solvent accessible surface area (SASA) during the simulation time (f).

3.2. Characterization of PC@QNs

3.2.1. Morphology

The color of the film plays a crucial role in shaping consumer preferences during product selection. As shown in Fig.S1, the incorporation of QNs imparted a bright yellow color to the PC composite film. The resulting PC@QNs film exhibited a smooth surface and maintained good optical transparency as observed by the naked eye, which is generally regarded as acceptable by consumer. Fig. 2a displayed the surface and cross-sectional SEM images of the PC@QNs films. The surface of pure PC composite film (PC) appeared smooth, and the addition of QNs had no obvious effect on the PC. In addition, a compact structure was observed on cross-sections of PC@QNs, with the increase in QNs content, the compactness became highly evident due to the more uniform dispersion within the film, indicating the high compatibility of PC matrix with QNs. In addition, the cross-sections of PC@QNs revealed a compact structure. With the increase in QNs content, the compactness became more pronounced due to the more uniform dispersion of QNs within the film, indicating the high compatibility between the PC matrix and QNs.

3.2.2. FTIR

FTIR spectroscopy was employed to analyze the interactions between QNs and the PC matrices. As presented in Fig. 2b, the FTIR spectra of PC film and PC@QNs films were similar, no additional peak was present after added QNs, indicating that no new chemical bonds were formed between the QNs and the PC matrix. A similar result had been reported in previous studies on the self-growth of quercetin crystals in cassia gum (Cao et al., 2020). The characteristic peaks at 3300 cm^{-1}, 2930 cm^{-1}, 1410 cm^{-1}, and 1030 cm^{-1} were attributed to O—H stretching vibrations, C—H stretching vibrations, O—H bending vibrations, and C—O stretching vibrations, respectively (Ning et al., 2024). With the addition of QNs, the characteristic peaks near 3300 cm^{-1} and 1410 cm^{-1} were shifted to varying degrees in the vicinity, which implied the formation of a denser hydrogen bond network between QNs and PC.

3.2.3. XRD

The crystallization characteristics and structure of PC@QNs were evaluated using X-ray diffraction, and the spectra are shown in Fig. 2c. The PC film exhibited a diffraction peak at 19.9°, showing a typical semi-crystalline structure (Chen et al., 2024). After the introduction of QNs, this diffraction peak intensified, indicating an increase in the crystallinity of the PC@QNs. This result could be attributed to the addition of QNs that facilitated the alignment and ordering of molecular chains. However, the peak at 19.9° for PC@QNs3 weakened and broadened, which may be attributed to the excessive QNs disrupting the original hydrogen bonds within the CS and PVA chains, resulting in the partial

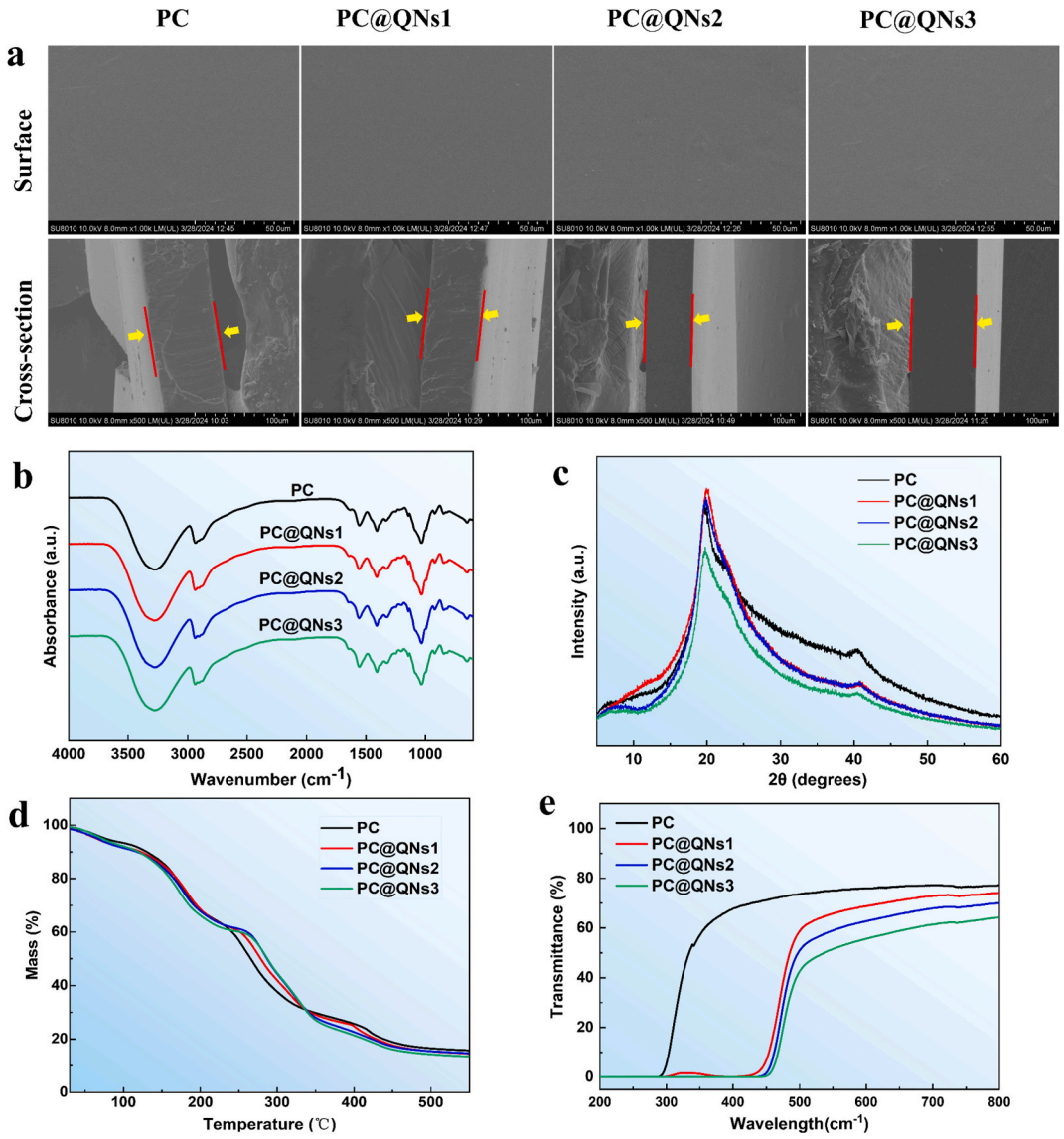

Fig. 2. Characterization of the quercetin nanocrystals (QNs) reinforced chitosan/ polyvinyl alcohol films (PC@QNs). Microscopic images of the surface and cross-section of the PC@QNs films (a), FTIR spectra (b), XRD spectra (c), thermal weight loss curve (d), and transmittance across a wavelength range of 200 to 800 nm (e). PC refers to chitosan/polyvinyl alcohol composite films without quercetin nanocrystals. PC@QN1, PC@QN2, and PC@QN3 refer to composite films containing 5 %, 10 %, and 15 % (*v*/v) QNs solution, respectively.

destruction of the crystalline structure. Some studies suggested that the crystallinity of the film is closely related to its mechanical properties (Cao et al., 2020; Ning et al., 2024; Zhao et al., 2024).

3.2.4. Thermal behavior

The thermal behavior of the films was analyzed using thermogravimetric analysis to investigate the effect of QNs additives on the PC films. As shown in Fig. 2d, all films exhibited three distinct stages of mass loss during the thermogravimetric analysis. The first stage occurred in the temperature range of approximately 120 °C, primarily due to the evaporation of water adsorbed in the films. The subsequent second stage, occurring around 280 °C, corresponded to the loss of bound water and the degradation of the PC polymer backbone. It is worth noting that the degradation degree of the films containing QNs was reduced during this stage, suggesting that the introduction of QNs improved the thermal stability of the PC films. The third stage of mass loss occurred in the range of approximately 450 °C, primarily due to the decomposition of residues.

3.2.5. Optical properties

Ultraviolet light accelerates the degradation of chemical bonds in polymers as well as lipid and protein oxidation, leading to the loss of mechanical properties in films and food deterioration (Kaschuk et al., 2022; Zhang & Jiang, 2023). UV light is typically categorized into UV-A (400–320 nm), UV-B (320–280 nm), and UV-C (280–200 nm). The light transmittance of the films across a selected wavelength range was measured to evaluate their optical properties. As shown in Fig. 2e, the PC film exhibited high transmittance in the wavelength range of 200–400 nm, whereas the transmittance of PC@QNs decreased to 0 %, implying that QNs improved the UV-blocking ability of the films. This critical role is attributed to the UV absorption capabilities of the benzene ring and specific phenolic hydroxyl groups in QNs. Moreover, a decrease in the transmittance of the films in the visible light region (600 nm) was observed with the increasing addition of QNs, which might be attributed to the enhanced light scattering caused by the QNs.

3.2.6. Mechanical properties

The mechanical properties of food packaging films determine their

suitability for various application scenarios, which can be quantitatively assessed by tensile strength for mechanical strength and elongation at break for ductility (Bai et al., 2024). The mechanical properties of PC and PC@QNs are shown in Fig. 3a. The tensile strength increased from 36.92 MPa to 49.68 MPa as the QNs content increased from 0 % to 10 %, representing a 34.56 % improvement compared to the PC film. However, it decreased when the QNs content exceeded 10 %, indicating that an appropriate amount of QNs incorporation enhances the mechanical strength of the PC film. The introduction of QNs into PC films initially reduced the elongation at break to 148.54 % ($P < 0.05$), followed by an increase to 176.02 %. The mechanical strength and ductility of PC@QNs3 surpass those of most biodegradable food packaging materials (Fig. 3b), indicating the advantages of the reinforcement strategy employed in this work. This phenomenon can be attributed to the role of QNs not merely as inert additives, but as structural enhancers that reinforce interfacial compatibility and polymer chain cohesion within the PC film. Moreover, their uniform dispersion and nanoscale dimensions enable them to function as physical cross-linking nodes, restricting polymer chain mobility and promoting chain entanglement during film formation (Zhang, He, et al., 2024) (Fig. 3c). After balancing the two key structural material properties, strength and malleable, QNs contribute positively to the mechanical properties of films.

3.2.7. MD simulations

To further explore the intermolecular interaction between QNs within the PC polymer network, the previous QNs (quercetin aggregates, in section 3.1.2), CS polymer chains, and PVA polymer chains were set in a box. Fig. 3d showed the motion trajectories of molecules and the evolution of the overall structure. Initially, the QNs (green), CS polymer chains (red), and PVA polymer chains (blue) were loosely distributed. As the simulation progressed, they gradually aggregated, indicating the formation of interactions. As presented in Fig. 3e, both electrostatic and van der Waals interactions were observed between QNs and the CS/PVA matrix, indicating that QNs interact with both CS and PVA components. This is consistent with the FTIR results, which revealed the formation of strong hydrogen bonds between QNs and the CS/PVA matrix, as hydrogen bonding is primarily a form of directional electrostatic interaction. Notably, the interaction energy between QNs and CS was more negative than that between QNs and PVA, suggesting a stronger interaction. This could be attributed to the electrostatic attraction between the negatively charged QNs and the positively charged amino groups of CS, along with the abundant hydroxyl groups, which provide a large number of binding sites for QNs through electrostatic interactions and hydrogen bonding.

3.3. WVP and OP

The water and oxygen barrier properties of packaging materials are crucial for maintaining food quality (Huang et al., 2023). As shown by the WVP values in Fig. 4a, the WVP of the films decreased from 10.62 to 8.21×10^{-12} g Pa^{-1} m^{-1} s^{-1} as the QNs content increased from 0 % to 15 %. Low WVP effectively blocks water transmission between food and

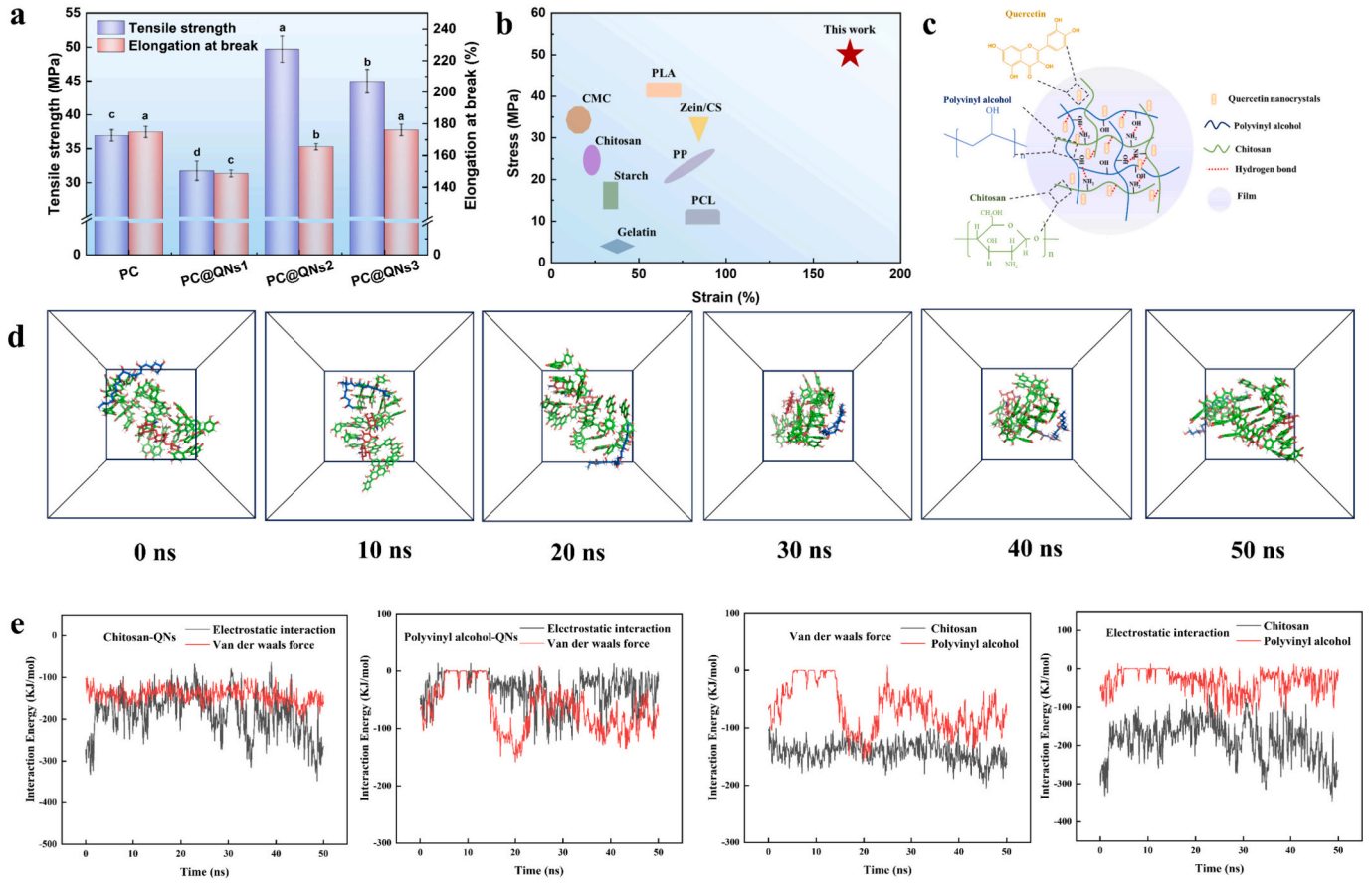

Fig. 3. Mechanical properties of the quercetin nanoparticles (QNs) reinforced chitosan/ polyvinyl alcohol films (PC@QNs). Tensile strength and elongation at break (a) and comparison with other food packaging materials (b) and schematic diagram of the mechanism of mechanical property enhancement (c). Molecular dynamics simulations of PC@QNs, structural changes of the system during the simulation (d), and binding energy of systems (e). PC refers to chitosan/polyvinyl alcohol composite films without quercetin nanocrystals. PC@QN1, PC@QN2, and PC@QN3 refer to composite films containing 5 %, 10 %, and 15 % (v/v) QNs solution, respectively.

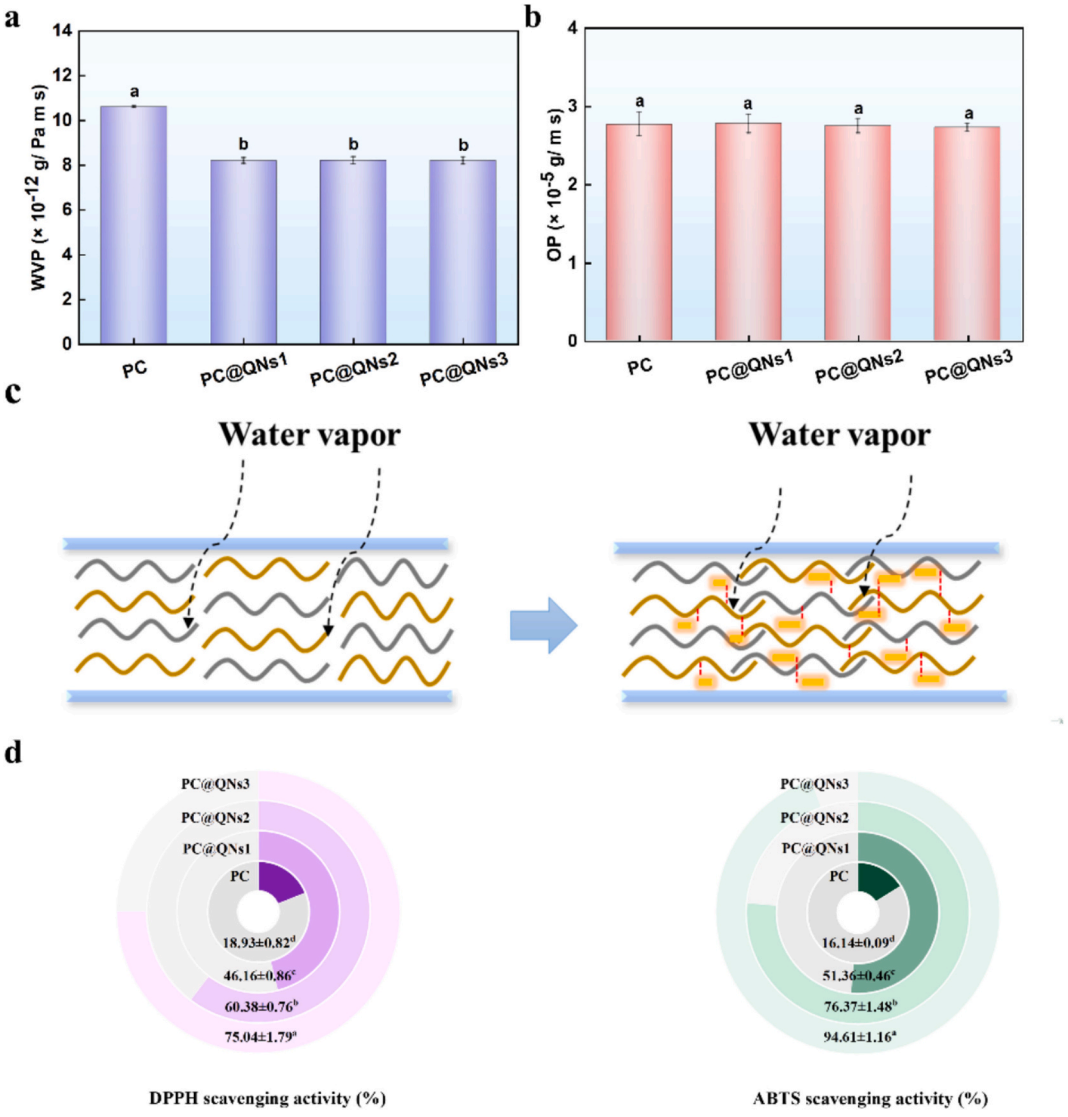

Fig. 4. Barrier properties of quercetin nanocrystals (QNs) reinforced chitosan/ polyvinyl alcohol films (PC@QNs). Water vapor permeability (a), oxygen permeability (b), and water vapor transmission path through the film (c). Antioxidant activity of PC@QNs, DPPH, and ABTS radical scavenging capacity. PC refers to chitosan/polyvinyl alcohol composite films without quercetin nanocrystals. PC@QN1, PC@QN2, and PC@QN3 refer to composite films containing 5 %, 10 %, and 15 % (v/v) QNs solution, respectively.

air, which is crucial for extending food shelf life. This reduction was attributed to the uniform dispersion of QNs within the PC matrix, which established interfacial interactions (e.g. hydrogen bond) between the nanofiller and polymer matrix, thereby limiting water molecule interactions and impeding moisture penetration. Moreover, the physical barrier effect of QNs generated tortuous diffusion pathways for water molecules, further impeding moisture penetration (Fig. 4c). However, the OP performance of PC@QNs showed no significant change ($P > 0.05$) (Fig. 4b). Some studies suggest that when molecular interactions between nanofillers and polymer chains are enhanced, the mobility of polymer chains is restricted, which could explain the insensitivity of PC@QNs films to oxygen barrier performance (Zhao et al., 2022).

3.4. Antioxidant properties

Oxidation is recognized as one of the primary factors contributing to food spoilage, particularly for foods with high fat content (Kuai et al., 2021). A 95 % (v/v) ethanol/water solution was used as a simulant for fatty foods (such as meat) to evaluate the antioxidative activity of the films. As shown in Fig. 4d, the PC film had a limited hydrogen donation capacity, resulting in the lowest DPPH free radical scavenging rate (18.93 ± 0.82 %) and ABTS free radical scavenging rate (16.14 ± 0.09 %), indicating poor antioxidant capacity. As expected, the DPPH radical scavenging rate (46.16 %–75.04 %) and ABTS radical scavenging rate (51.36 %–94.61 %) of the films containing QNs were markedly higher ($P < 0.05$), demonstrating a concentration dependent trend with increasing QNs content. This enhancement in antioxidant capacity is attributed to the phenolic hydroxyl groups in QNs, which are capable of scavenging free radicals directly through hydrogen atom donation (Masek et al., 2018).

3.5. Environmental impact

The environmental impact of PC@QNs was assessed in comparison to traditional polypropylene (PP) and polyethylene (PE) films, with a focus on the perspective of raw materials (J.-D. Wang, et al., 2024). As shown in Fig. 5a, the PC@QNs1 film demonstrated a 63.11 % reduction in fossil resource scarcity compared with the same mass of PE film. Additionally, global warming potential and fine particulate matter formation were reduced by 28.03 % and 23.77 %, respectively.

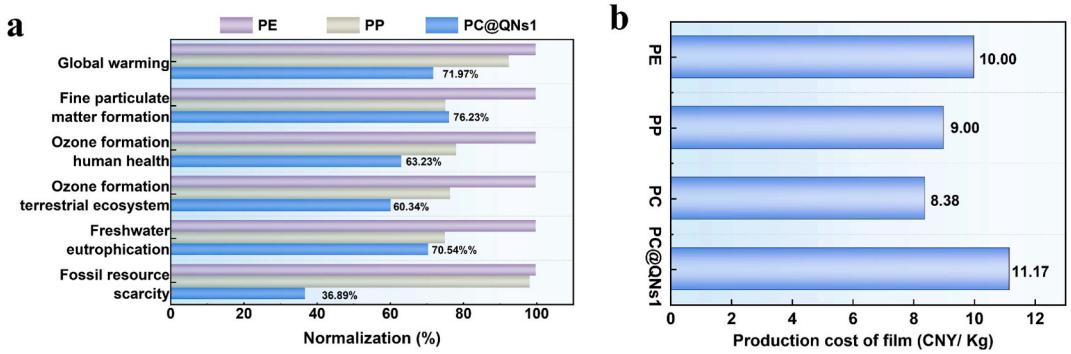

Fig. 5. Environment impact (a) and material cost of producing quercetin nanocrystals (QNs) reinforced chitosan/ polyvinyl alcohol films (PC@QNs) (b). PC@QN1 refers to composite films containing 5 % (v/v) QNs solution.

Furthermore, ozone formation impacts on human health and the terrestrial ecosystem were reduced by more than 40 %. These analyses underscore the sustainability of PC@QNs films, which integrate biodegradable components and natural additives, providing an eco-friendly alternative to traditional petroleum-based packaging materials like PE films. For industrial production considerations, the material cost of the PC@QNs was calculated in Fig. 5b. The material cost of producing 1 kg of PC@QNs film was 11.7 % higher than that of producing 1 kg of PE film. However, due to its outstanding performance in food preservation and reduction in environmental impact, the PC@QNs film demonstrated significant potential for large-scale production and application as a sustainable packaging alternative.

3.6. *Application in meat preservation*

Due to the balanced excellent performance of PC@QNs2 in mechanical properties, barrier properties and antioxidant activity, PC@QNs2 was selected to carry out the meat preservation experiment. To evaluate the preservation performance of PC@QNs2, the morphology changes over different storage periods, along with key shelf-life indicators such as TVC and TVB-N, were analyzed. As shown in Fig. 6a, changes were observed in the meat packaged with different films over

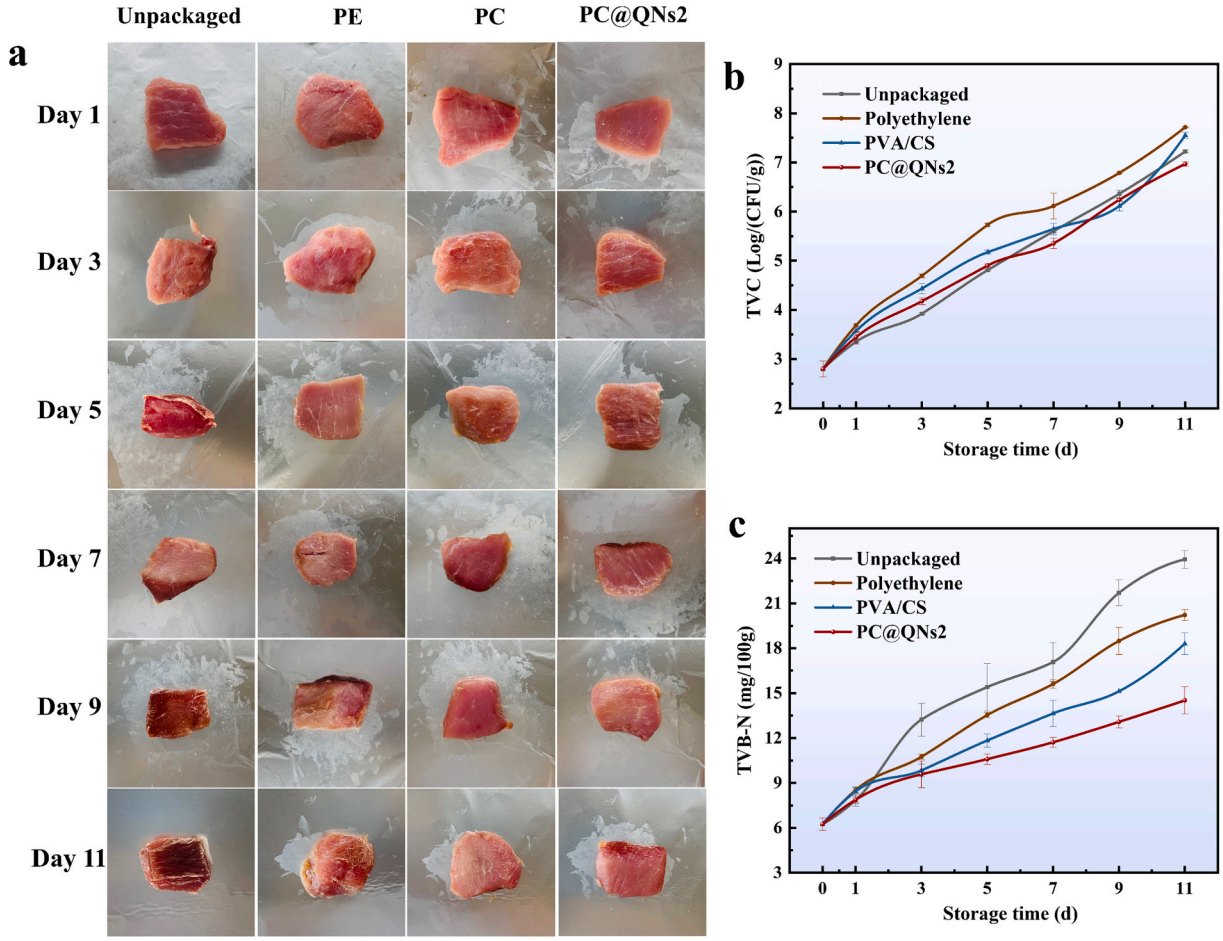

Fig. 6. Application of film in meat preservation. The visual appearance of meat (a), total viable count (TVC)(b), and total volatile basic nitrogen analysis (TVB-N) (c) changes during storage. PC refers to chitosan/polyvinyl alcohol composite films without quercetin nanocrystals. PC@QN2 refers to composite films containing 10 % (v/v) QNs solution.

increasing storage times. In the unpackaged group, the surface of the meat gradually darkened and became stiff. The meat in the PE film-packaged group became cloudy and slimy over a longer period, emitting a decayed odor. Conversely, the meat packaged with PC@QNs2 film maintained a clear texture and firm structure even after an extended period, indicating that PC@QNs film effectively prolongs the shelf life of meat.

Meat spoilage is closely associated with bacterial proliferation (Wen et al., 2022). The degree of spoilage in packaged meat was evaluated by measuring the TVC (Fig. 6b). The TVC value of the PC@QNs film group consistently remained lower than that of the other groups. At the end of storage (day 11), the TVC value for the PC@QNs film group was 6.97 log CFU/g, significantly lower than those of the unpackaged group (7.22 log CFU/g) and the PE film group (7.72 log CFU/g). These results suggested that bacterial growth was slower in the meat packaged with PC@QNs film. TVB-N is a widely used indicator of protein degradation and spoilage in fresh meat. It mainly comprises ammonia, trimethylamine, and dimethylamine, which are produced by microbial metabolism and enzymatic breakdown of nitrogen-containing compounds during storage (Bekhit et al., 2021; Gu et al., 2023). As shown in Fig. 6c, the initial TVB-N value of the meat was approximately 6.24 mg/100 g. As time progressed, the TVB-N value of the unpackaged group and the PE film group increased sharply to 23.94 mg/100 g and 20.22 mg/100 g, respectively. Notably, the TVB-N of the meat packaged with the PC@QNs film slowly increased, which was valued at 14.51 mg/100 g at the end of storage, showing a satisfactory result. According to above results, the PC@QNs film effectively prolonged the shelf life of meat to 11 days. The excellent preservation performance of PC@QNs can be attributed to the synergistic antimicrobial and antioxidant activities of QNs, which effectively inhibit microbial growth and retard oxidative degradation during storage. Specifically, when the QNs-containing film is applied to the surface of fresh meat, QNs gradually release from the film to the meat surface. There, they exert antimicrobial effects by disrupting bacterial cell structures and interfering with metabolic processes, thereby suppressing the proliferation of spoilage microorganisms (Li et al., 2023). In addition, QNs contribute to oxidative stability by scavenging free radicals and chelating metal ions, thus reducing lipid and protein oxidation throughout storage. Despite the promising preservation effects of PC@QNs, the safety of the film material requires further investigation to enhance its acceptability for food packaging applications. Overall, the developed film provides a protective microenvironment that delays spoilage, extends shelf life, and maintains product quality.

4. Conclusions

In this study, QNs were successfully prepared through self-assembly and used to enhance the functionality of PC composite film. Results from MD simulation and characterizations revealed that the self-assembly of QNs was primarily driven by various supramolecular interactions, including π-π stacking, hydrogen bonds, and electrostatic interactions. QNs exhibit good compatibility with PC composite films. The addition of QNs significantly enhances the mechanical properties (with a tensile strength of 49.68 MPa and an elongation at break of 176.02 %), UV-blocking ability (with 0 % transmittance), and water vapor barrier performance (with a 22.69 % reduction) of PC composite films. Moreover, the PC@QNs3 film exhibited a fourfold increase in antioxidant activity compared to the plain PC film. When applied to pork meat packaging, the PC@QNs2 effectively delayed the rise in TVC and TVB-N, extending the fresh meat's shelf life to 11 days. Compared to previously reported nanoparticles used in biopolymer films, the QNs in this study offer the advantage of being fully active, self-assembled structures with both functional bioactivity and structural enhancement capability, leading to synergistic improvements in film performance. Overall, this study provides an effective strategy for fabricating eco-friendly and functional food packaging materials, utilizing QNs both as nanofillers and bioactive agents to improve the properties of PC composite films.

CRediT authorship contribution statement

Simin Fan: Writing – original draft, Methodology. **Wenxin Wang:** Writing – review & editing, Data curation. **Qingfeng Yang:** Methodology, Investigation. **Chaoqiao Zhu:** Formal analysis, Data curation. **Ming Tian:** Software, Methodology, Investigation. **Aurore Richel:** Writing – review & editing, Supervision. **Marie-Laure Fauconnier:** Writing – review & editing, Supervision. **Chengli Hou:** Writing – review & editing, Resources, Project administration. **Dequan Zhang:** Writing – review & editing, Supervision, Resources.

Declaration of competing interest

The authors declare that they have no known competing financial interests or personal relationships that could have appeared to influence the work reported in this paper.

Acknowledgments

This work was supported by the National Key Research and Development Program of China (No. 2024YFD2101600), and the Program of China Scholarship Council (No. 202303250065). We appreciated Phadcalc (www. phadcalc.com) for the molecular dynamics simulation.

Appendix A. Supplementary data

Supplementary data to this article can be found online at https://doi.org/10.1016/j.foodchem.2025.145826.

Data availability

Data will be made available on request.

References

Bai, H., Yang, L., Wu, L., Xiao, D., & Dong, A. (2024). Enhanced food preservation platform integrating photodynamic and chemical antibacterial strategies via geraniol-loaded porphyrin-based MOFs for cherry tomato storage. *Chemical Engineering Journal, 498*, Article 155503.

Bekhit, A. E.-D. A., Holman, B. W. B., Giteru, S. G., & Hopkins, D. L. (2021). Total volatile basic nitrogen (TVB-N) and its role in meat spoilage: A review. *Trends in Food Science & Technology, 109*, 280–302.

Cao, L., Feng, H., Meng, F., Li, J., & Wang, L. (2020). Fabrication of a high tensile and antioxidative film via a green strategy of self-growing needle-like quercetin crystals in cassia gum for lipid preservation. *Journal of Cleaner Production, 266*, Article 121885.

Chen, X., Lan, W., & Xie, J. (2024). Characterization of active films based on chitosan/polyvinyl alcohol integrated with ginger essential oil-loaded bacterial cellulose and application in sea bass (Lateolabrax japonicas) packaging. *Food Chemistry, 441*, Article 138343.

Chenxi, Z., Hemmat, A., Thi, N. H., & Afrand, M. (2025). Nanoparticle-enhanced drug delivery systems: An up-to-date review. *Journal of Molecular Liquids, 424*, Article 126999.

Fan, S., Wang, D., Wen, X., Li, X., Fang, F., Richel, A., Xiao, N., Fauconnier, M.-L., Hou, C., & Zhang, D. (2023). Incorporation of cinnamon essential oil-loaded Pickering emulsion for improving antimicrobial properties and control release of chitosan/gelatin films. *Food Hydrocolloids, 138*, Article 108438.

Fan, S., Yang, Q., Zhu, C., Li, X., Richel, A., Fauconnier, M.-L., Fang, F., Zhang, D., & Hou, C. (2024). Zein/chitosan Janus film incorporated with tannic acid and cinnamon essential oil co-loaded Pickering emulsion for sustained controlled release and pork preservation. *International Journal of Biological Macromolecules, 138429*.

Fu, S., Yi, X., Li, Y., Li, Y., Qu, X., Miao, P., & Xu, Y. (2024). Berberine and chlorogenic acid-assembled nanoparticles for highly efficient inhibition of multidrug-resistant Staphylococcus aureus. *Journal of Hazardous Materials, 473*, Article 134680.

Gu, M., Li, C., Su, Y., Chen, L., Li, S., Li, X., Zheng, X., & Zhang, D. (2023). Novel insights from protein degradation: Deciphering the dynamic evolution of biogenic amines as a quality indicator in pork during storage. *Food Research International, 167*, Article 112684.

Guo, X., Luo, W., Wu, L., Zhang, L., Chen, Y., Li, T., Li, H., Zhang, W., Liu, Y., Zheng, J., & Wang, Y. (2024). Natural products from herbal medicine self-assemble into advanced bioactive materials. *Advanced Science, 11*(35), 2403388.

He, T., Niu, N., Chen, Z., Li, S., Liu, S., & Li, J. (2018). Novel quercetin aggregation-induced emission Luminogen (AIEgen) with excited-state intramolecular proton transfer for in vivo bioimaging. *Advanced Functional Materials, 28*(11), 1706196.

Hu, Y., Miao, Y., Zhang, Y., Wang, X., Liu, X., Zhang, W., & Deng, D. (2024). Co-assembled binary polyphenol natural products for the prevention and treatment of radiation-induced skin injury. *ACS Nano, 18*(40), 27557–27569.
Huang, H.-D., Ren, P.-G., Zhong, G.-J., Olah, A., Li, Z.-M., Baer, E., & Zhu, L. (2023). Promising strategies and new opportunities for high barrier polymer packaging films. *Progress in Polymer Science, 144*, Article 101722.
Jiang, S., Qiao, C., Liu, R., Liu, Q., Xu, J., & Yao, J. (2023). Structure and properties of citric acid cross-linked chitosan/poly(vinyl alcohol) composite films for food packaging applications. *Carbohydrate Polymers, 312*, Article 120842.
Kandemir, K., Tomas, M., McClements, D. J., & Capanoglu, E. (2022). Recent advances on the improvement of quercetin bioavailability. *Trends in Food Science & Technology, 119*, 192–200.
Kaschuk, J. J., Al Haj, Y., Rojas, O. J., Miettunen, K., Abitbol, T., & Vapaavuori, J. (2022). Plant-based structures as an opportunity to engineer optical functions in next-generation light management. *Advanced Materials, 34*(6), 2104473.
Kuai, L., Liu, F., Chiou, B.-S., Avena-Bustillos, R. J., McHugh, T. H., & Zhong, F. (2021). Controlled release of antioxidants from active food packaging: A review. *Food Hydrocolloids, 120*, Article 106992.
Li, F., Zhe, T., Ma, K., Zhang, Y., Li, R., Cao, Y., Li, M., & Wang, L. (2023). One stone two birds: Multifunctional flavonol nanocrystals enable food packaging to both preserve freshness and visually monitor freshness. *Chemical Engineering Journal, 453*, Article 139760.
Luo, J., Luo, J., Sheng, Z., Fang, Z., Fu, Y., Wang, N., Yang, B., & Xu, B. (2025). Latest research progress on anti-microbial effects, mechanisms of action, and product developments of dietary flavonoids: A systematic literature review. *Trends in Food Science & Technology, 156*, Article 104839.
Ma, K., Zhe, T., Li, F., Zhang, Y., Yu, M., Li, R., & Wang, L. (2022). Sustainable films containing AIE-active berberine-based nanoparticles: A promising antibacterial food packaging. *Food Hydrocolloids, 123*, Article 107147.
Manca, M. L., Lai, F., Pireddu, R., Valenti, D., Schlich, M., Pini, E., … Sinico, C. (2020). Impact of nanosizing on dermal delivery and antioxidant activity of quercetin nanocrystals. *Journal of Drug Delivery Science and Technology, 55*, Article 101482.
Masek, A., Latos, M., Piotrowska, M., & Zaborski, M. (2018). The potential of quercetin as an effective natural antioxidant and indicator for packaging materials. *Food Packaging and Shelf Life, 16*, 51–58.
Ning, Y., Yang, W., Liu, S., Xu, J., Cheng, X., Xu, S., Li, J., & Wang, L. (2024). A fluorescent polyvinyl alcohol film with efficient photodynamic antimicrobial performance enabled by Berberine/Phytic acid salt for food preservation. *Advanced Functional Materials, n/a(n/a)*, 2411314.
Ning, Y., Yang, W., Liu, S., Xu, J., Cheng, X., Xu, S., Li, J., & Wang, L. (2025). A Fluorescent Polyvinyl Alcohol Film with Efficient Photodynamic Antimicrobial Performance Enabled by Berberine/Phytic Acid Salt for Food Preservation. *Advanced Functional Materials, n/a*(n/a), Article 2411314.
Peydayesh, M., Kovacevic, A., Hoffmann, L., Donat, F., Wobill, C., Baraldi, L., … Mezzenga, R. (2024). Sustainable smart packaging from protein Nanofibrils. *Advanced Materials, n/a(n/a)*, 2414658.
Priyadarshi, R., Roy, S., Ghosh, T., Biswas, D., & Rhim, J.-W. (2022). Antimicrobial nanofillers reinforced biopolymer composite films for active food packaging applications - a review. *Sustainable Materials and Technologies, 32*, Article e00353.
Shlush, E., & Davidovich-Pinhas, M. (2022). Bioplastics for food packaging. *Trends in Food Science & Technology, 125*, 66–80.
Sultan, M., Youssef, A., & Baseer, R. A. (2024). Fabrication of multifunctional ZnO@ tannic acid nanoparticles embedded in chitosan and polyvinyl alcohol blend packaging film. *Scientific Reports, 14*(1), 18533.
Thakur, S., Chaudhary, J., Sharma, B., Verma, A., Tamulevicius, S., & Thakur, V. K. (2018). Sustainability of bioplastics: Opportunities and challenges. *Current Opinion in Green and Sustainable Chemistry, 13*, 68–75.
Uysal-Unalan, I., Sogut, E., Realini, C. E., Cakmak, H., Oz, E., Espinosa, E., … Corredig, M. (2024). Bioplastic packaging for fresh meat and fish: Current status and future direction on mitigating food and packaging waste. *Trends in Food Science & Technology, 152*, Article 104660.
Wang, D., Chen, J., Wen, X., Fan, S., Zhu, C., Li, X., Fang, F., Yang, W., Fan, W., Zhang, D., & Hou, C. (2024). Self-assembled chitosan/polyvinyl alcohol hydrogel film incorporated with TiO2 with excellent stability, mechanical and antibacterial properties for the preservation of chilled pork. *Food Packaging and Shelf Life, 45*, Article 101328.
Wang, J., & Zhuang, S. (2022). Chitosan-based materials: Preparation, modification and application. *Journal of Cleaner Production, 355*, Article 131825.
Wang, J.-D., Yang, S.-L., Liu, G.-S., Zhou, Q., Fu, L.-N., Gu, Q., Cai, Z.-H., Zhang, S., & Fu, Y.-J. (2024). A degradable multi-functional packaging based on chitosan/silk fibroin via incorporating cellulose nanocrystals-stabilized cinnamon essential oil Pickering emulsion. *Food Hydrocolloids, 153*, Article 109978.
Wang, X., Xue, J., Wang, Y., Zhu, H., Chen, S., Xiao, Z., & Luo, Y. (2024). Development and characterization of zein/gum Arabic nanocomposites incorporated edible films for improving strawberry preservation. *Advanced Composites and Hybrid Materials, 7*(6), 249.
Wang, Z., Lu, J., Yuan, Z., Pi, W., Huang, X., Lin, X., Zhang, Y., Lei, H., & Wang, P. (2023). Natural carrier-free binary small molecule self-assembled hydrogel synergize antibacterial effects and promote wound healing by inhibiting virulence factors and alleviating the inflammatory response. *Small, 19*(5), 2205528.
Wen, X., Zhang, D., Li, X., Ding, T., Liang, C., Zheng, X., Yang, W., & Hou, C. (2022). Dynamic changes of bacteria and screening of potential spoilage markers of lamb in aerobic and vacuum packaging. *Food Microbiology, 104*, Article 103996.
Yang, D., Liu, Q., Gao, Y., Wan, S., Meng, F., Weng, W., & Zhang, Y. (2023). Characterization of silver nanoparticles loaded chitosan/polyvinyl alcohol antibacterial films for food packaging. *Food Hydrocolloids, 136*, Article 108305.
Yang, W., Zhang, S., Feng, A., Li, Y., Wu, P., Li, H., & Ai, S. (2024). Water-insoluble tea polyphenol nanoparticles as fillers and bioactive agents for pectin films to prepare active packaging for fruit preservation. *Food Hydrocolloids, 156*, Article 110364.
Zhang, L., He, W., Ping, Y., Wang, W., Hu, P., Li, B., Zhu, W., Sun, J., Ji, Y., & Wang, J. (2024). Autonomous, temperature-enhanced oxidase-mimic multimodal antimicrobial film for prolonged preservation of perishable products. *Chemical Engineering Journal, 491*, Article 152116.
Zhang, W., Khan, A., Ezati, P., Priyadarshi, R., Sani, M. A., Rathod, N. B., … Rhim, J.-W. (2024). Advances in sustainable food packaging applications of chitosan/polyvinyl alcohol blend films. *Food Chemistry, 443*, Article 138506.
Zhang, Y., & Jiang, W. (2023). Effective strategies to enhance ultraviolet barrier ability in biodegradable polymer-based films/coatings for fruit and vegetable packaging. *Trends in Food Science & Technology, 139*, Article 104139.
Zhao, X., Chen, Z., Zhuo, H., Zhong, C., Shi, G., Liu, T., Huang, X., Zhong, L., & Peng, X. (2024). Ultra-strong and transparent biomimetic nanocomposite through orientation effects and in situ biomineralization. *Advanced Functional Materials, 34*(1), 2310094.
Zhao, Y., Zhou, S., Xia, X., Tan, M., Lv, Y., Cheng, Y., Tao, Y., Lu, J., Du, J., & Wang, H. (2022). High-performance carboxymethyl cellulose-based hydrogel film for food packaging and preservation system. *International Journal of Biological Macromolecules, 223*, 1126–1137.